Conf-891192--31

WSRC-RP--89-499

DE92 009940

ANALYSIS OF NATURAL CONVECTION IN A WASTE GLASS MELTER

by

Inn Gui Choi

Westinghouse Savannah River Company
Savannah River Site
Aiken, SC 29808
803-725-6362

A paper proposed for presentation at the
Annual Westinghouse Corporate Computer Symposium
Pittsburgh, PA
November 6-7, 1989

and for publication in the proceedings

Analysis of Natural Convection in a Radioactive Waste Glass Melter

by

Inn G. Choi

Westinghouse Savannah River Site
Savannah River Laboratory
Aiken, SC 29808-0001
(803) 725-6362

Abstract

Laminar natural convection in a two-dimensional cavity with a line heat sink at the top boundary is investigated numerically. The fluid in the cavity is a high Prandtl number fluid with volumetric heat source. Parametric study is conducted to find the effect of variations in Rayleigh number, aspect ratio, sink location, and volumetric heat source on the flow and temperature field.

better to incorporate (HLW) in glass

1. Introduction

A concerted effort is under way at the Savannah River Site (SRS) to convert liquid radioactive waste into ~~an immobile~~ glass product. The radioactive waste and glass-forming material (frit) are mixed at high temperatures (1150° C) to form a homogeneous glass.

A large amount of work has been done on determining the properties of waste glass under various conditions, but less efforts have been spent on predicting the behavior of glass motion and its effects on homogeneity. Occurrences of cold and hot spots within the mixture are known to exist during melting, but they are difficult to determine experimentally.

A commercial fluid dynamics code, FIDAP [1], is used to determine the characteristics of glass melt convection under various conditions. A two-dimensional model is adequate for this purpose. More elaborate three-dimensional modeling efforts to couple the full momentum, energy, and electric equations are currently under way.

A sketch of one of the pilot-scale radioactive waste glass melters in SRS is shown in Figure 1. High-level radioactive waste is vitrified by feeding waste slurry into the glass melter. The slurry covers most of the top surface area of the molten pool in the melter. This slurry layer, which is called cold cap, is heated from below by the glass melt via Joule-heating and from above by radiation from dome heaters in the plenum.

The electrode configuration for this melter ~~have~~ has shown relatively uniform current density field [2] in the melter under a normal operating condition. Therefore, the effect of Joule-heating can be accounted for by providing a uniform volumetric heat source to the melt without sacrificing too much accuracy.

The cold cap can be considered ~~as~~ (to be) a heat sink [3] whereas the remaining melt surface opened to the plenum a heat source. Thus the base case can be identified as a Rayleigh-Bernard type of natural convection problem in a cavity with a heat sink and source along the top boundary.

2. Governing Equations

The problem of interest can be described mathematically by the continuity equation, Navier-Stokes equations as modified by the Boussinesq approximation, and the energy equation with volumetric heat source. The equations are written in a vector form as

$$\nabla \mathbf{u} = 0$$

$$\rho \mathbf{u} \, \nabla \mathbf{u} = -\nabla p + \rho g \beta T + \mu \nabla^2 \mathbf{u}$$

$$\rho C_p \mathbf{u} \, \nabla T = k \nabla^2 T + q_s$$

These equations assume a steady state flow of an incompressible fluid with volumetric heat generation and with negligible viscous dissipation. The variables are defined as

$\mathbf{u}$ = velocity (m/sec)
T = temperature (°C)
x, y = coordinates (m)
μ = viscosity (N-sec/m^2)
C_p = specific heat (joules/k_g°K)
k = conductivity (watts/m °K)
β = volume expansion coefficient (°K^{-1})
g = gravity (m/sec^2)
ρ = density (k_g/m^3)
α = thermal diffusivity (m^2/sec)
q_s = volumetric heat generation (joule/sec m^3)

Introducing the following nondimensional variables,

$\mathbf{u}^* = \mathbf{u}/\mathbf{U}$
$T^* = (T-T_r)/(T_2 - T_r)$
$x^* = x/L$
$p^* = pL/\mu\mathbf{U}$
$q^* = q/Q$

where

$\mathbf{U} = \alpha\sqrt{R_a P_r}/L$
$Q = k\Delta T/L$

and

Rayleigh number, $R_a = \rho\beta g(T_2 - T_1)L^3/\mu\alpha$
Prandtl number, $P_r = \nu/\alpha = \mu C_p/k$

the continuity, momentum, and energy equations can be written, dropping asterisks, as

$$\nabla \mathbf{u} = 0$$

$$\sqrt{R_a/P_r}\, \mathbf{u}\, \nabla \mathbf{u} = -\nabla p + \nabla^2 \upsilon + \sqrt{R_a/P_r}\, T_e$$

$$\sqrt{R_a/P_r}\, \mathbf{u}\, \nabla T = \nabla^2 T + q_s$$

3. Base Case

The two-dimensional cross section of the melter that is being considered in this study is one-half of the symmetric plane of the glass melt volume across each pair of the electrodes. In Figure 2, this glass melt volume is shown with the upper and lower recesses occupied by these electrodes. The waste slurry dropped from the top is melted and carried away from the cavity through an opening located on the sidewall near the bottom floor. However, the effect of this opening on the overall convection field has been found to be small(2). Therefore the cavity is assumed to be completely closed for this problem.

The boundary conditions for the base case are displayed in Figure 2. It is assumed that the top boundary is subject to a heat sink ($0. < x < 0.7$) and a heat source ($0.7 < x < 0.8$). For the bottom boundary, a constant temperature boundary condition is used. The wall to the left is a symmetric adiabatic plane. The wall to the right is assumed to lose heat by a constant amount of heat flux.

Figure 3 compares the calculated results with experimental data. The experimental data were obtained from the DWPF Scale Glass Melter in SRS, and are presented here to show the general shape of the vertical temperature distribution. The experimental data show fuller parabolic profile with steeper temperature gradients in the upper and lower region. Largest uncertainties in the measured data take place at the top boundary as anticipated.

Shown in figure 4 are the velocity vectors and isotherms for the base case. The most dominant convection currents take place at the mid-height location between the upper and lower electrodes. The maximum nondimensional velocity is 0.015 which is equivalent to 0.93 mm/sec. These convection currents are basically Rayleigh-Bernard type, and produced primarily by unstably stratified vertical thermal gradients. The effect of the isothermal source-sink at the top boundary is manifested by a mild secondary circulation at the upper-left corner. This indicates that the flow field at this Rayleigh number is not fully unstable.

The isotherms are closely spaced and nearly horizontal. The energy is transferred by the isothermal core at the center and by the heat source at the upper-right corner into the region between the two electrodes. The glass is entrained upward into the thermal boundary layer at a nearly uniform rate to compensate this energy. In the lower half region, the flow motion is resisted due to the stable thermal gradients. As the result, the temperature gradient in this region is almost linear.

4. Parametric Study

The motivation for this parametric study was to obtain a better understanding of the mixing mechanism induced by the natural convection current. The major parameters involved are Rayleigh number, aspect ratio, sink location, and heat generation. The effect of heat sink location and volumetric heat generation on the flow field is an important aspect from modeling point of view. Temperature and velocity profiles are presented for each case.

(1) Rayleigh number

The Rayleigh number was varied in the range, 2.9×10^4 - 6.5×10^6. This range includes all the convective motions possible in the typical glass melt temperature range, 1000°C - 1150°C. In this temperature range, the melt viscosity decreases by a factor of four and the conductivity increases by a factor of two to three with increasing temperature, whereas other properties remain relatively constant. Since the viscosity change is most severe and its square is inversely proportional to buoyancy force, a slight temperature change in the melt can produce a large change in the consequent flow motion.

The possible variations of the convective motion in the Rayleigh number range described above are shown in the streamline plots in Figure 5. For each of the plots in this figure, the primary flow in the lower-right region moves clockwise, whereas the secondary flow in the upper-left region moves counter-clockwise.

Initially, at $R_a = 2.9\times10^4$, the flow is marginally stable. When Rayleigh number increases, the flow becomes increasingly unstable. The size of the secondary circulation cell proportionally grows until it occupies almost one-half of the entire melt pool cavity as shown for the case of $R_a = 6.5\times10^6$ in the lower-right side corner in Figure 5. At this Rayleigh number, the primary circulation cell breaks up, and tertiary cells start to appear.

Rayleigh number increase also results in thinning of the thermal boundary layer as shown in the isotherm plots in Figure 6. At $Ra=6.5x10^6$, an extremely thin boundary layer develops all around the cavity wall. In the center, however, a large isothermal core region develops.

(2) Aspect Ratio

The two aspect ratios used in this study represent two experimental melter configurations existing in the Savannah River Site. These two melters are identical in all dimensions except the diameter of the glass melt volume that differs by a factor of two. Therefore, the amount of volumetric heat generation and sidewall heat losses to be assigned to the model should be different. The input values for each model were deduced from the available experimental data.

The streamline and isotherm plots are shown in Figure 7 and 8. The streamline plots indicate that, when the cavity width decreases, the secondary circulation cell at the upper-left corner disappears. This is because the buoyancy force decreases proportionally to the cubic of the characteristic length which is the cavity width in this case. Therefore a small reduction in the cavity width will make the relative magnitude of the buoyancy force drop significantly with respect to the viscous force, thus stabilizing the flow.

The isotherm plots in Figure 8 show that, for the narrower cavity, the vertical temperature profile is almost linear for the entire melt volume except the region at the top. The thinned thermal boundary layer along the top boundary and sidewall is evident. These isotherms are typical for a stable flow in a cavity.

(3) Location of Sink

The top boundary between the glass melt and cold cap is difficult to define because fusion, melting, and chemical reaction is taking place simultaneously. The simplest way to define this boundary is to assume that it is a heat sink. In an idle condition of the melter, however, it can also be a heat source because, in this case, the slurry is not fed and the top surface is directly exposed to the radiation from the dome heaters.

From this perspective, the three cases, namely, a sink ($T=-0.5$), a sink ($T=-0.5$) and source ($T=1.0$), and a source ($T=1.0$) along the top boundary were compared. The bottom boundary was fixed at $T=0.0$. The results are shown in Figure 9. The streamlines show that the secondary circulation diminishes when the top boundary changes from a sink to a source because the source at the top tends to stabilizes the flow.

The stable thermal stratification that can be achieved when the top boundary temperature is higher than the bottom is clearly shown in Figure 10. From mixing point of view, the presence of instability in the flow field is preferred because multiple cells promote heat transfer.

(4) Heat Generation

Volumetric heat generation by Joule-heating is the major heating mechanism of the waste glass. Without it, it will be extremely difficult to raise melt temperature level because the waste glass is basically a poor conductor. Figure 11 compares the vertical temperature profiles for the case where the internal heat generation is kept and the case where it is removed.

When the heat generation is present, the vertical temperature becomes fully parabolic with steep temperature gradients near the top. These steep temperature gradients are the results of heating the fluid layer located directly below the heat sink. The secondary flow motion in the upper region is created by these gradients. In the center, a relatively large isothermal core region is created. The top and bottom boundary interacts each other only through this core region.

When the heat generation is not present, the top and bottom boundary interact directly each other. Since the waste glass is a relatively poor heat conductor, the overall melt temperature level remains relatively low, and the heating of the fluid is confined in a small layer in the bottom. The consequence of the poor conduction heat transfer near the bottom is manifested by the kink in the vertical temperature profile at $x = 0.6$ as shown in Case D in Figure 11. This kink is the result of not being able to transport heat effectively.

Away from the bottom layer, the heat transfer is slightly enhanced due to a mild convection. In the region near the left boundary, Case (C) in Figure 11, however, the buoyancy force recovers its dominance over the viscous force. As the result, the temperature kink is stretched out, thus making the temperature profile more linear.

5. Applications

In general, a uniform flow is the primary flow driven by pressure gradient to transfer glass from one end to the other. Natural convection flow is a secondary flow that does not produce a net flow in any direction. In commercial glass furnace operation, the secondary flow motion might be created by batch charging, gas bubbles, and glass pull in addition to natural convection. In a waste glass melter, however, natural convection is the only source of a secondary flow motion.

From mixing point of view, glass melt uniformity can be achieved most effectively by creating multiple convective motions. Since multiple convective motions result from flow instability produced by unstable thermal stratification, it is necessary to have a warmer fluid at the bottom to create such an instability.

The fluid layer below the cold cap always remains unstable because its temperature is always substantially lower than the waste slurry temperature at the top. In the region under the cold cap, multiple oscillatory convective motions have been observed experimentally as well as numerically [4,5]. These motions, however, are confined within a small region of the upper layer.

For the primary convection currents, heating the bottom layer of the glass melt may be considered as the most direct and effective way of achieving glass uniformity. This is especially so for the waste glass because of the strong dependence of its viscosity on temperature. The magnitude of the primary convection can be increased by proper power skewing of the electrodes. When sufficiently high temperature gradients are produced, it is possible to produce even some active tertiary convection cells.

6. Conclusion

Laminar natural convection in a two-dimensional cavity with a line heat sink at the top boundary is investigated numerically. The fluid in the cavity is a high Prandtl number fluid with volumetric heat source.

The parametric study showed that the secondary convective motion resulting from flow instability is enhanced by increasing Rayleigh number and decreasing aspect ratio. At $R_a = 6.5 \times 10^6$, the flow becomes highly unstable and the secondary convection cell grows to the size of the primary cell. This secondary convection cell disappears when the aspect ratio increases by a factor of two.

The volumetric heat generation in the fluid medium contributes to increasing the overall temperature level and also to creating the secondary convective motion. For the latter, however, the presence of a heat sink at the top boundary is required to produce an unstably stratified thermal boundary layer.

References

(1) Fluid Dynamics International, Inc., "Fluid Dynamics Analysis Program", 1984

(2) Eyler, L. L. and Jones, E. O., "Scale Glass Melter Analysis of Freeze/Restart with TEMPEST Computer Code with Coupled Electric Field", ESD-89-100, 1989

(3) Clomburg, Jr., "Convection in an Enclosure-Source and Sink Located along a Single Horizontal Boundary", ASME-AIChE Heat Transfer Conference, St. Louis, Mo., 1976

(4) Eyler, L. L., et. al. "Physical and Numerical Modeling of Joule-Heated Melters", PNL-5491, UC-70, 1985

(5) Curlet, N. W. E., et. al. "Experimental and Mathematical Modeling of Three-Dimensional Natural Convection in an Enclosure, AIChE J., Vol. 30, No. 2, 1984, pp. 249-254

ACKNOWLEDGMENT

The information contained in this paper was developed under Contract No. DE-AC09-88SR18035 with the U. S. Department of Energy.

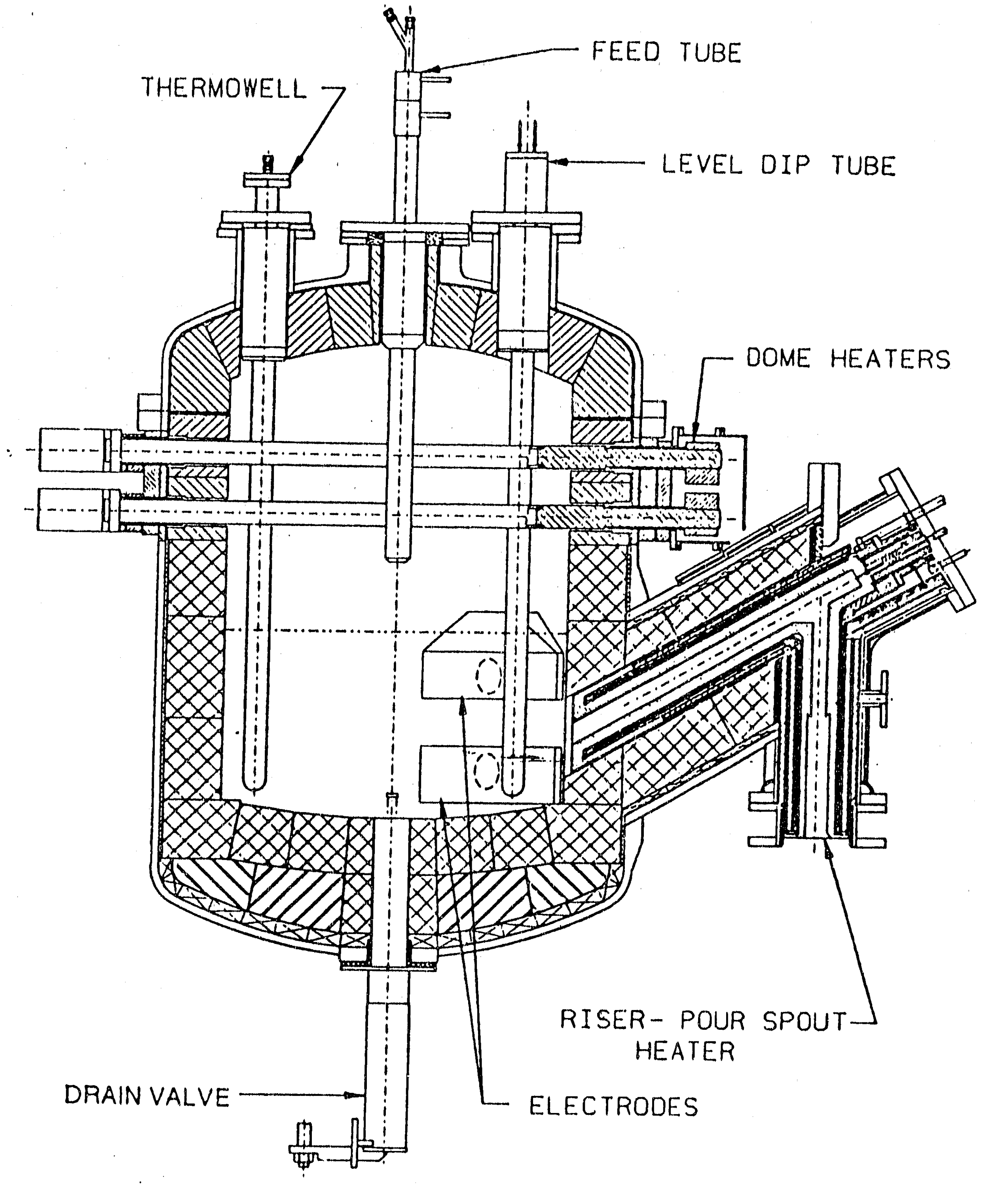

Figure 1. DWPF Scale Glass Melter

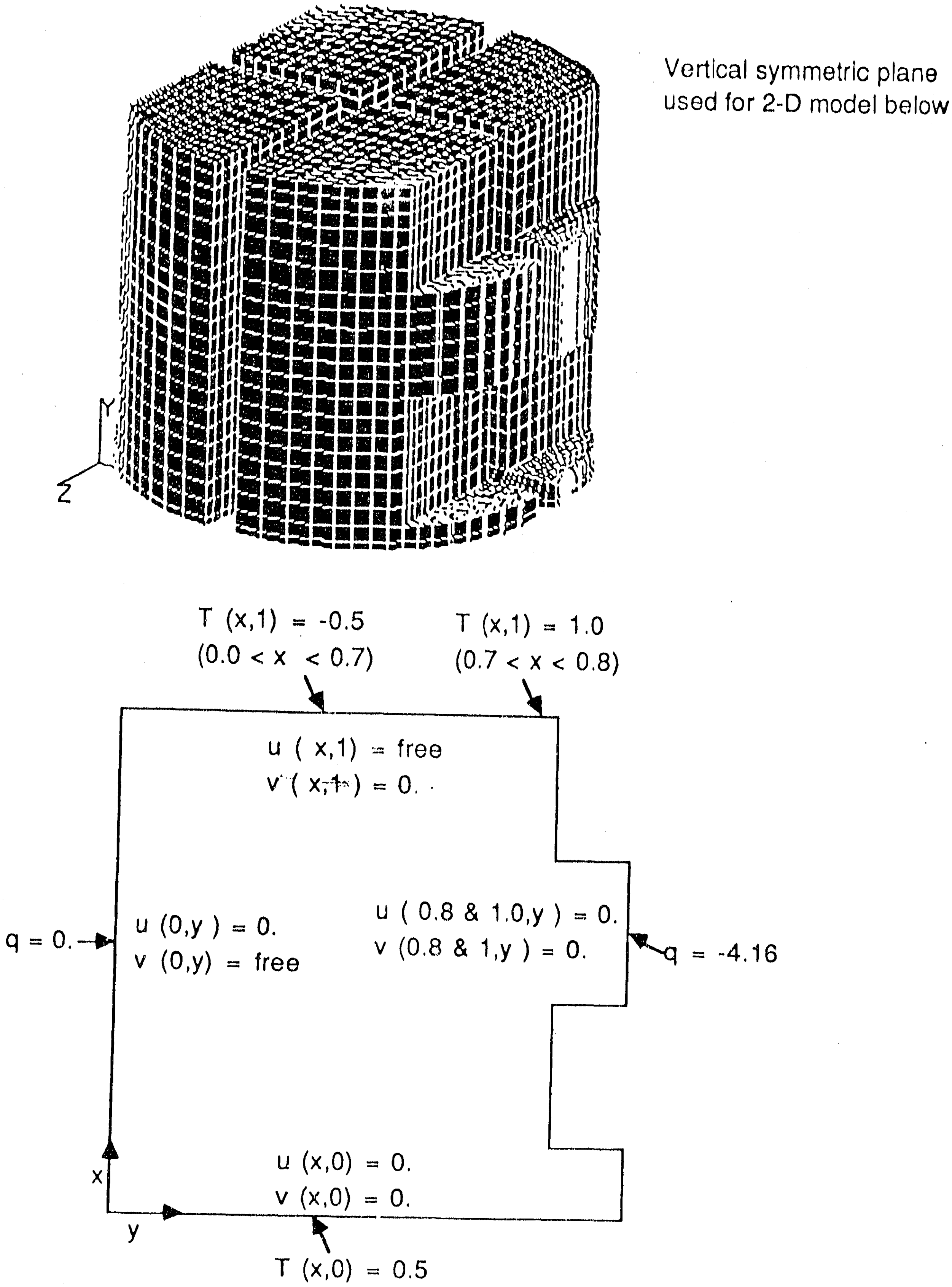

Figure 2. 2-D Melter Model Boundary Conditions

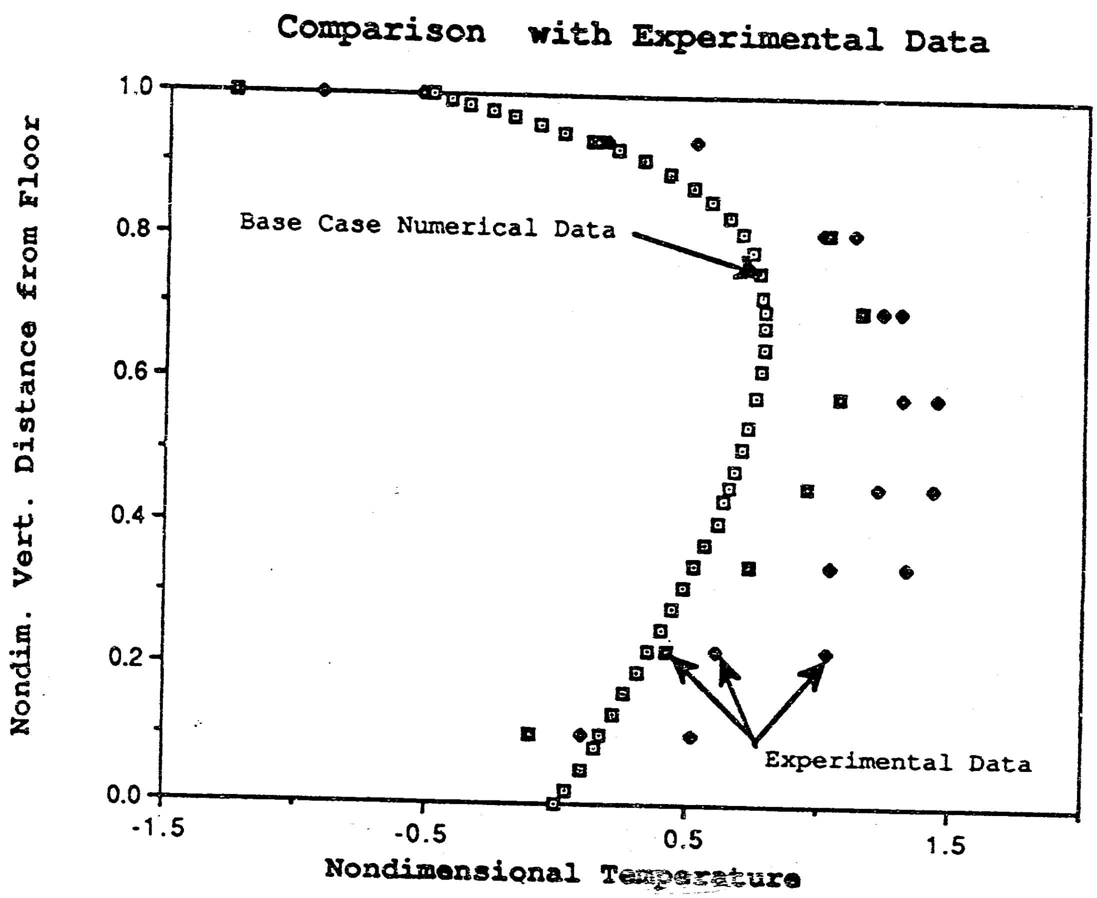

Figure 3. Comparison of 2-D Model Base Case with SGM Experimental Data

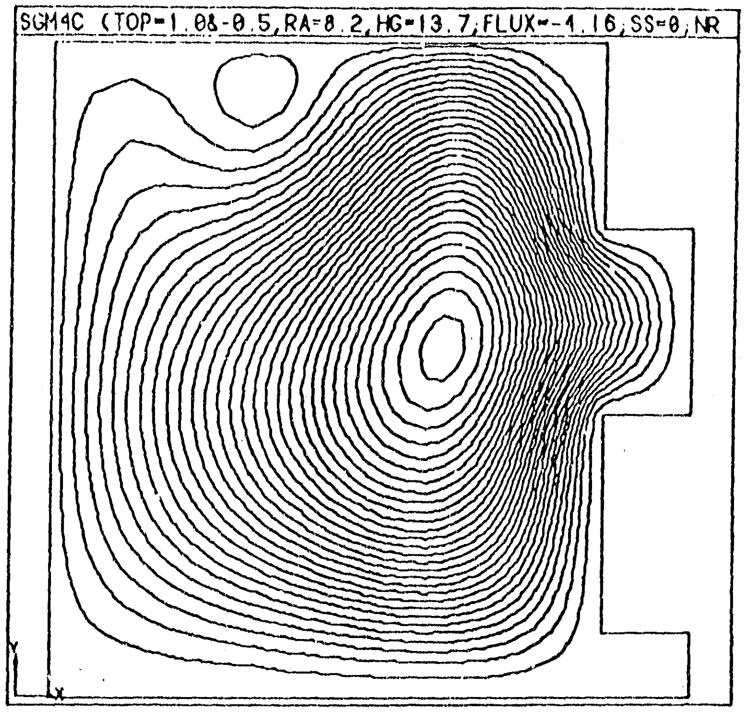

(A) Streamlines

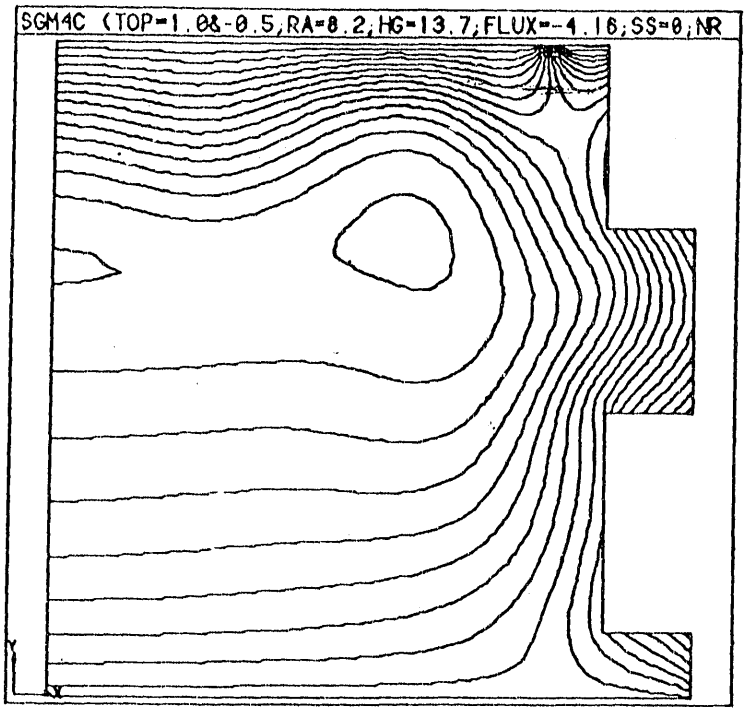

(B) Isotherms

Figure 4. Base Case Solutions

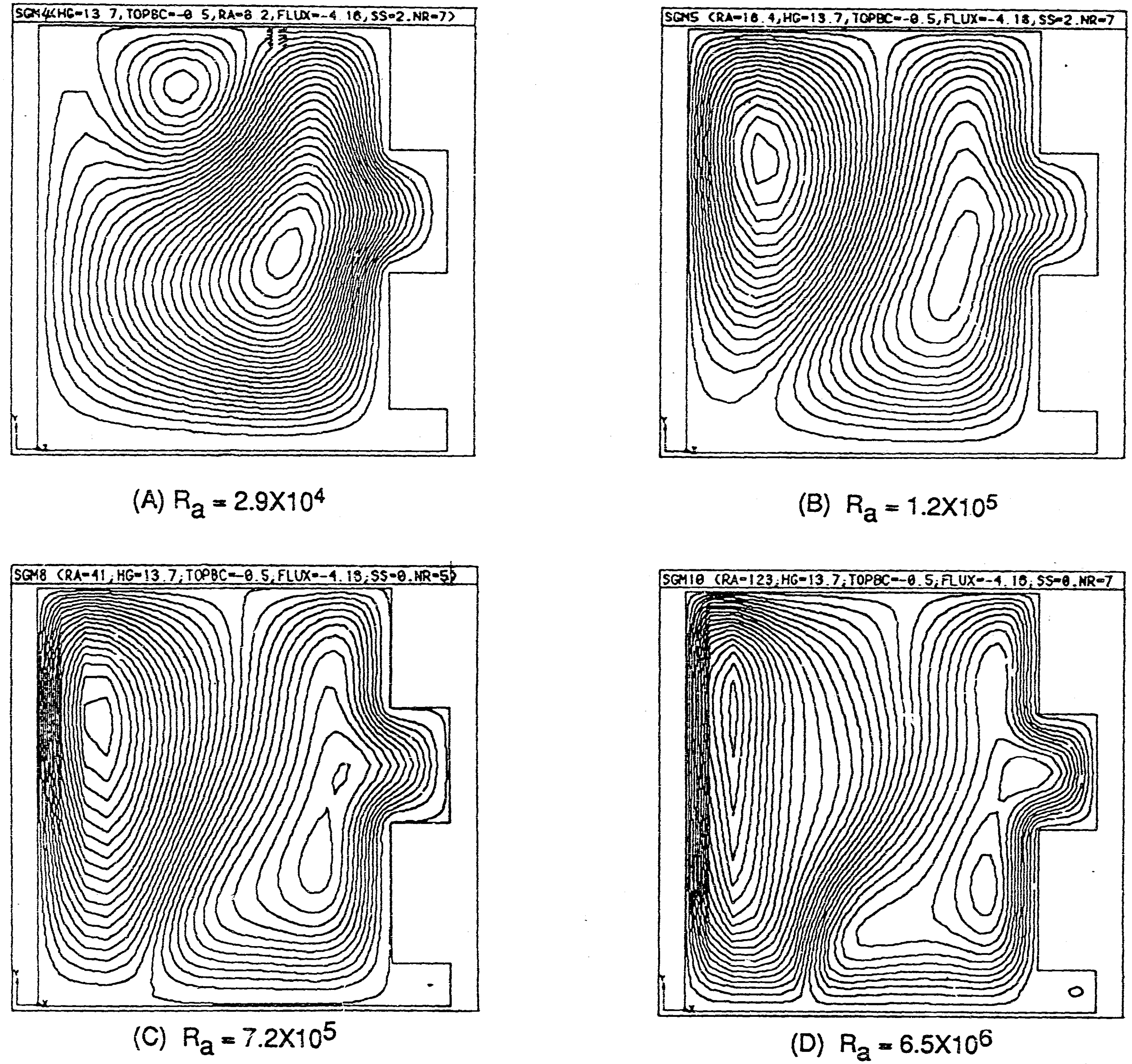

Figure 5. Effect of Rayleigh Number (Streamlines)

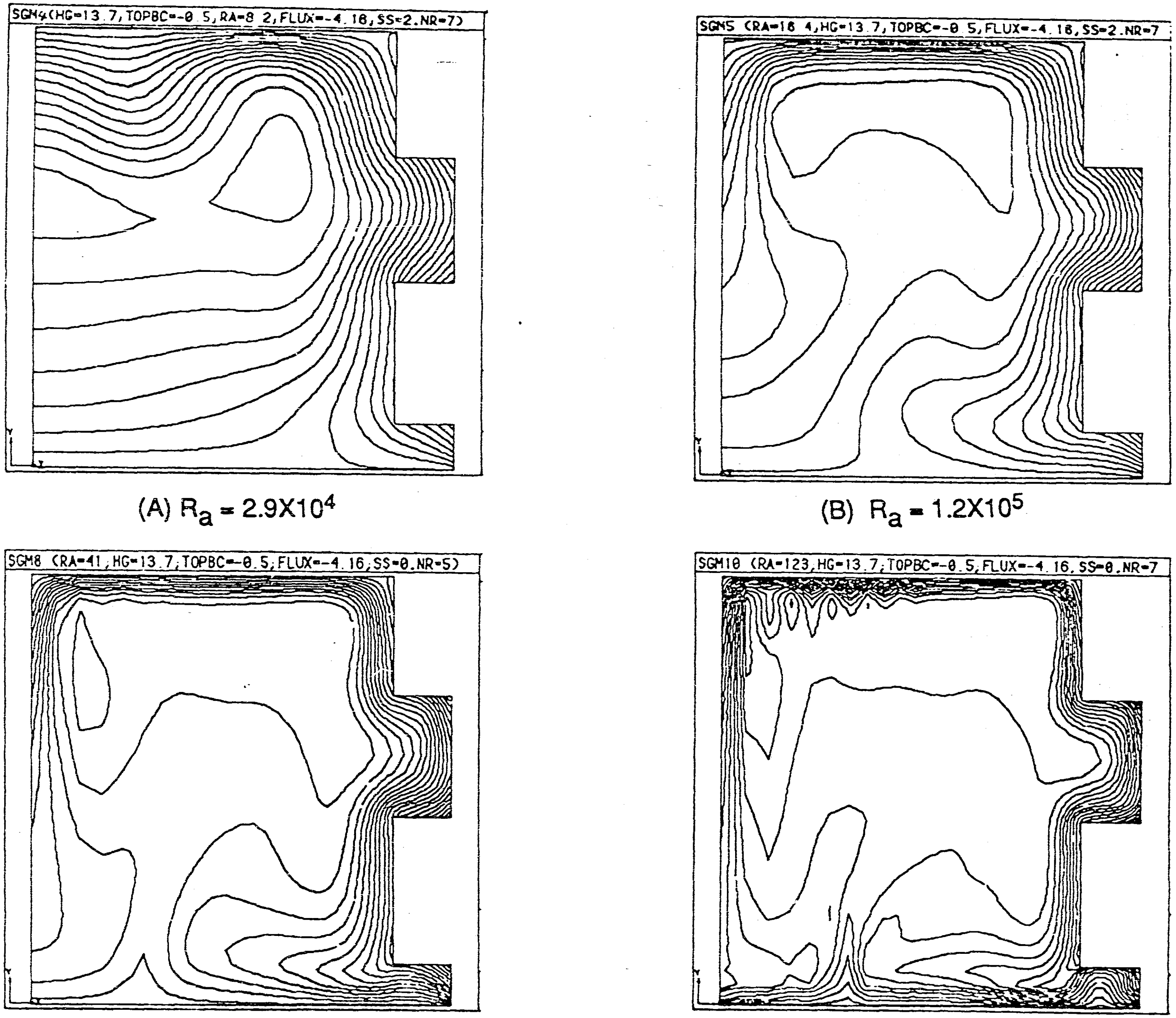

(A) $R_a = 2.9 \times 10^4$

(B) $R_a = 1.2 \times 10^5$

(C) $R_a = 7.2 \times 10^5$

(D) $R_a = 6.5 \times 10^6$

Figure 6. Effect of Rayleigh Number (Isotherms)

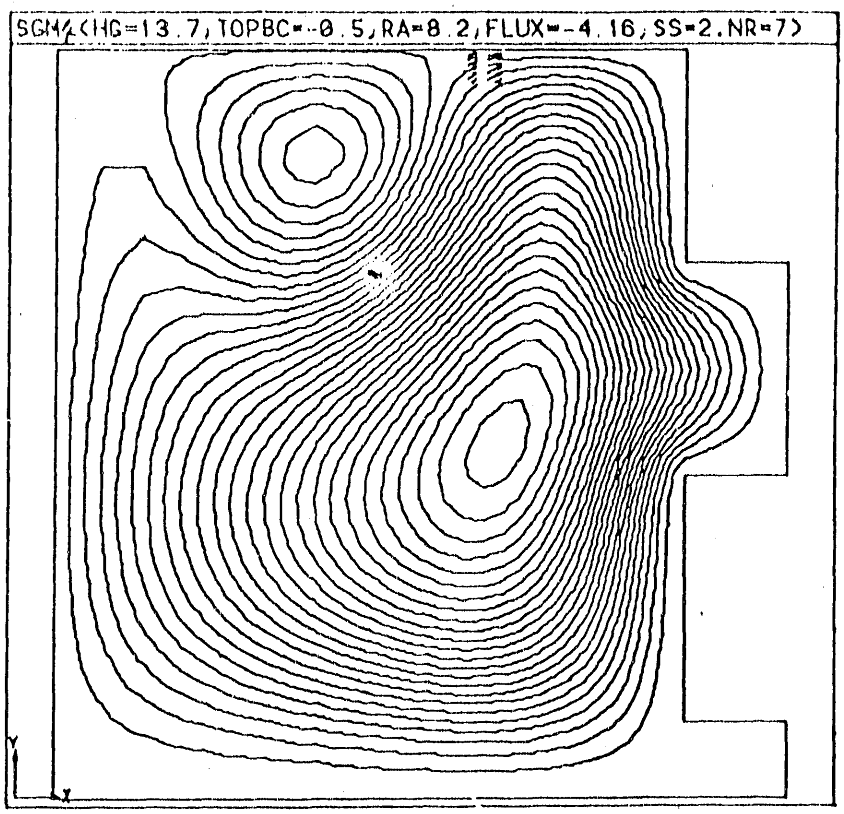

(A) Aspect Ratio = 1

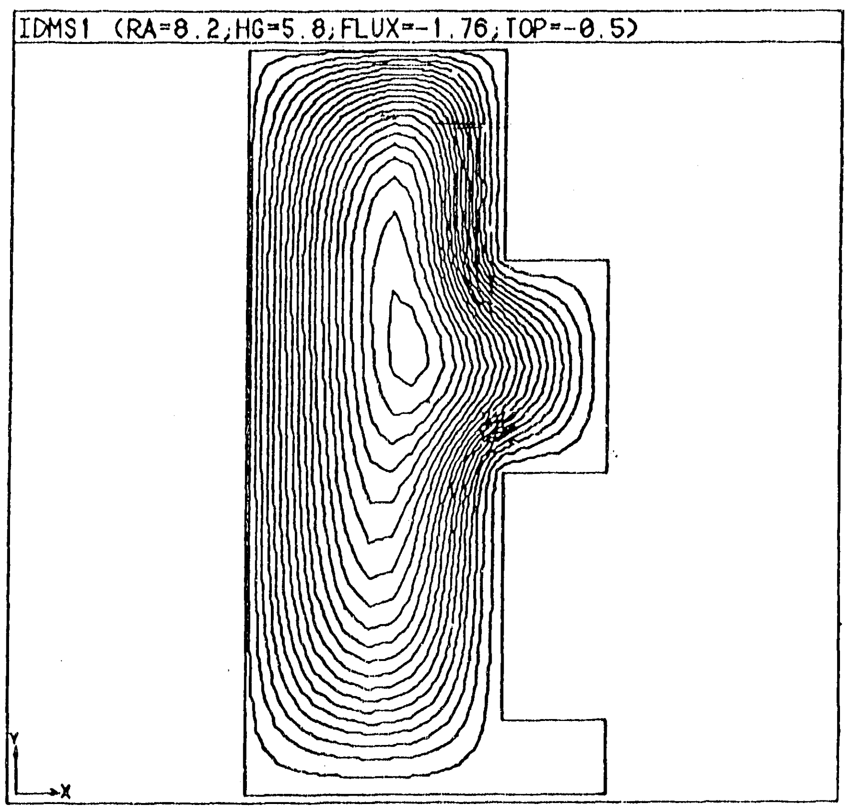

(B) Aspect Ratio = 2

Figure 7. Effect of Aspect Ratio (Streamlines)

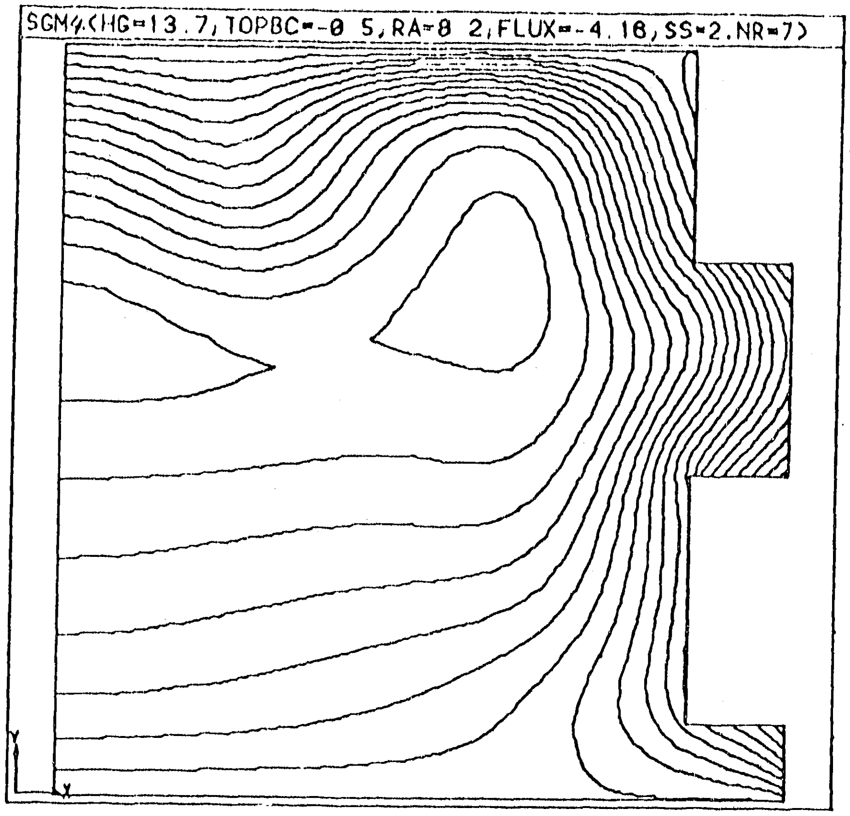

(A) Aspect Ratio = 1

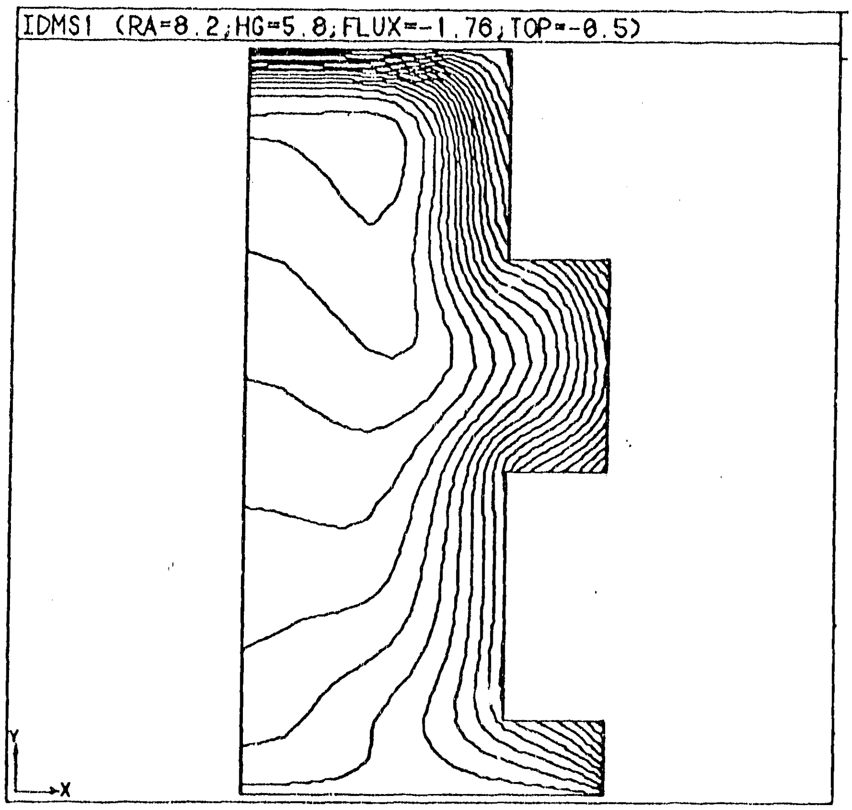

(B) Aspect Ratio = 2

Figure 8 Effect of Aspect Ratio (Isotherms)

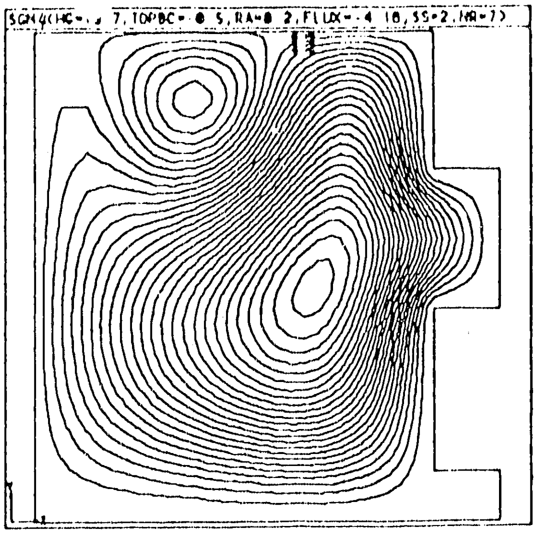

(A) Sink : -0.5 at 0.0< x <0.8

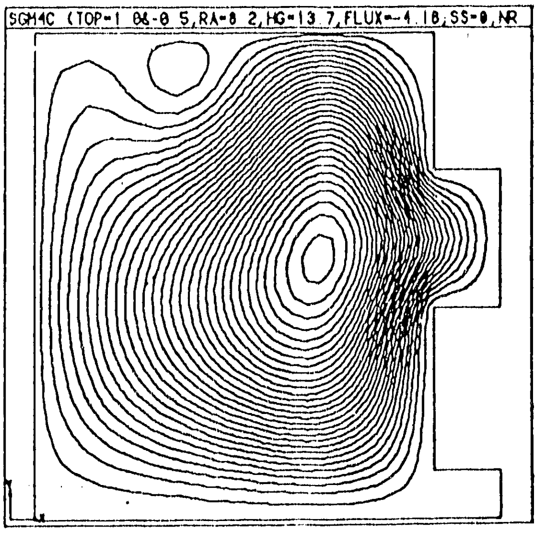

(B) Sink : -0.5 at 0.0< x <0.7 ; Source : 1.0 at 0.7< x <0.8

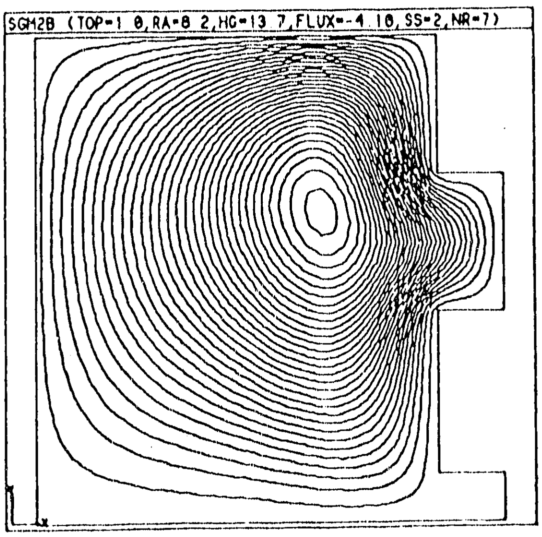

(C) Source : 1.0 at 0.0< x <0.8

Figure 9. Effect of Heat Sink/Source Location at Top Boundary (Streamlines)

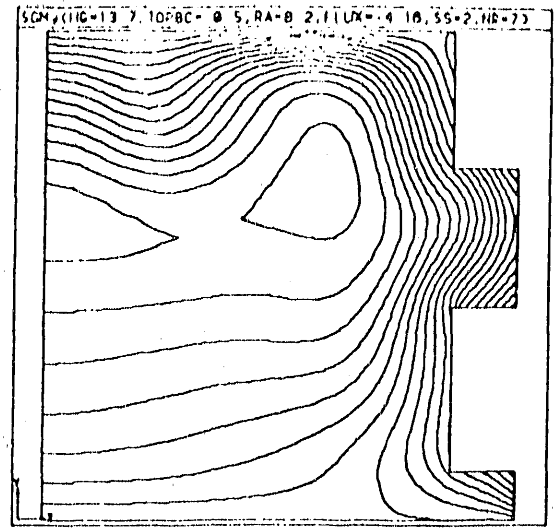

(A) Sink : -0.5 at 0.0< x <0.8

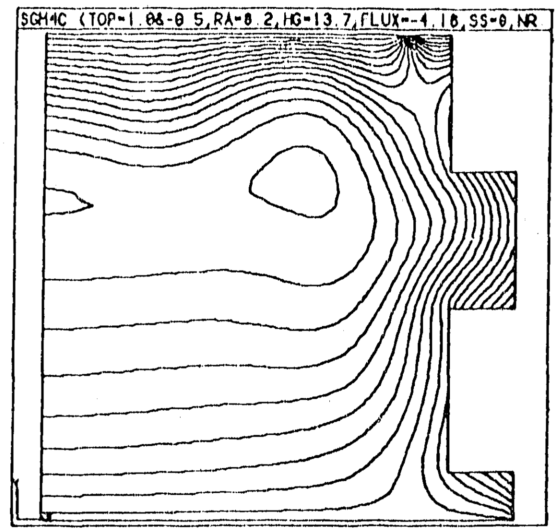

(B) Sink : -0.5 at 0.0< x <0.7 ; Source : 1.0 at 0.7< x <0.8

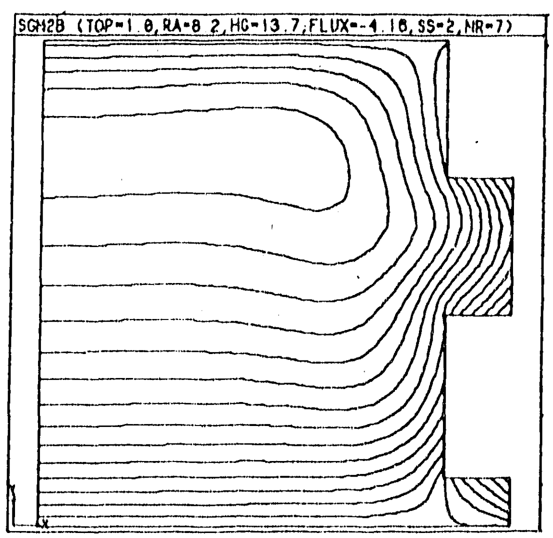

(C) Source : 1.0 at 0.0< x <0.8

Figure 10. Effect of Heat Sink/Source Location at Top Boundary

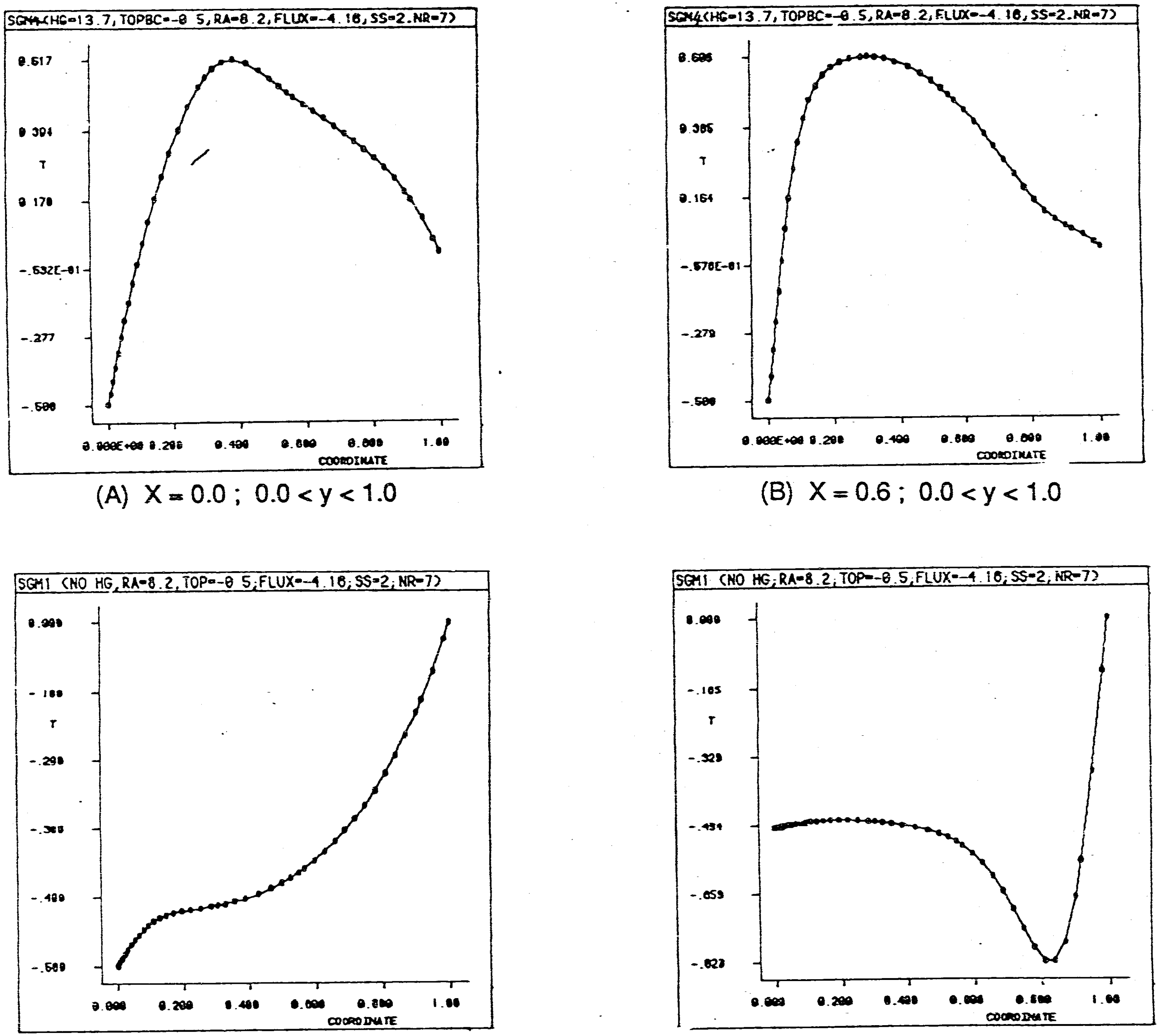

(A) X = 0.0 ; 0.0 < y < 1.0

(B) X = 0.6 ; 0.0 < y < 1.0

(C) X = 0.0 ; 0.0 < y < 1.0

(D) X = 0.6 ; 0.0 < y < 1.0

Figure 11. Effect of Volumetric Internal Heat Generation
(Top : With H.G. ; Bottom : Without H.G.)

END

DATE FILMED

4 / 27 / 92